Thermodynamic Modelling of the Fe-Al-Ti-O System and Evolution of Al-Ti Complex Inclusions during Ti-added Ultra Low Carbon Steel Production

Y.-J. Park[1] and _Y.-B. Kang_[2]

1. Ph.D candidate, Pohang University of Science and Technology, Pohang, Gyeongbuk, Rep. of Korea, 37673. Email: yjpark92@postech.ac.kr
2. Professor, Pohang University of Science and Technology, Pohang, Gyeongbuk, Rep. of Korea, 37673. Email: ybkang@postech.ac.kr

ABSTRACT

Ti-added Ultra-Low C (ULC) steel is produced by adding Al and Ti during the secondary refining process to deoxidize molten steel and to bind C and N which are detrimental to the deep drawing quality of the steel product. However, the production of Ti-added ULC steel faces challenges, including submerged entry nozzle clogging and surface defects on cold rolled coils. The troubles were often attributed to "Al-Ti complex inclusions" in the molten steel. However, the evolution of oxide inclusions including their stability has been still unclear. In the present study, the evolution of these inclusions in Ti-added ULC steel was investigated by phase diagram measurement, CALPHAD thermodynamic modelling, high-temperature stability test for the oxides, and observation of transient behaviour of oxide inclusions in the steel. The phase diagram of the Al-Ti-O system was elucidated with an emphasis on oxygen potential, which significantly controls the stability of the oxides. CALPHAD thermodynamic models and a self-consistent database were developed. The transient behaviour of Al-Ti complex inclusions in Ti-added ULC steel was observed _in-situ_ using a confocal scanning laser microscope. This was additionally validated by the new thermodynamic model. The equilibrium phases of the oxide inclusions were investigated using a high-temperature resistance furnace, and were analysed using a secondary electron microscope, energy dispersive spectrometer, and electron back-scattered diffraction. By considering the morphology and crystal structure of these inclusions, the evolution of Al-Ti oxide inclusions was elucidated. Various behaviour of Al-Ti inclusions and their influence on steel cleanliness are discussed.

1. INTRODUCTION

Interstitial-free (IF) steel, also known as Ultra-Low Carbon (ULC) steel, is widely used in automotive outer panels due to its excellent Deep Drawing Quality (DDQ). In order to further enhance the DDQ, IF steel requires minimizing interstitial elements such as C and N to the utmost extent. In particular, Ti is one of the most commonly used elements for improving the properties of IF steel. The addition of Ti has several beneficial effects, such as an increase in the plastic strain ratio (_r_-value), a decrease in the recrystallization temperature, and reduced sensitivity to coiling temperatures (Gupta and Bhattacharya (1989), Fukuda (1973)). As a result, the demand and supply of Ti-added ULC steel have been consistently increasing due to its excellent performance in maximizing DDQ properties.

During the production of Ti-added ULC steel, the steel undergoes deoxidation in the RH (Ruhrstahl-Heraeus) process by adding Al: $2\underline{Al} + 3\underline{O} = Al_2O_3(s)$. Subsequently, Ti is added as Ti sponge or ferro-Ti alloy to achieve the target composition. While Ti-free ULC steel only considers Al_2O_3 oxide as the non-metallic inclusion, in the case of Ti-added ULC steel, Ti may also react with dissolved O. This could happen if the Al deoxidation was not enough to kill the O or reoxidation occurs during the secondary refining or continuous casting processes. This may induce Ti-containing inclusions and further, Al-Ti complex inclusions. It has been reported that Ti-added ULC steel encounters more severe Submerged Entry Nozzle (SEN) clogging during continuous casting, compared Ti-free ULC steel (Basu _et al._ (2004), Cui _et al._ (2009), Lee _et al._ (2019)). The accumulation of clogging deposits

becomes more significant with increasing Ti content, resulting in poor productivity (Dorrer *et al.* (2019), Bernhard *et al.* (2019)).

The origin of the severe SEN clogging due to Ti addition includes refractory-steel reaction, reoxidation from various sources (air aspiration, Ar gas quality, refractory carbothermic reaction, etc.), enhanced wettability, etc. In addition to this, the evolution of inclusions by Ti addition may play a significant role, however, the phase stability of Al-Ti complex inclusions is yet to be understood clearly. Frequently mentioned oxide phase as the Al-Ti complex inclusion has been "Al_2TiO_5" and there have been cases where Al_2TiO_5 was observed in Ti-added ULC steel melts (Wang *et al.* (2009), Bai *et al.* (2019)). Several oxide stability diagrams of the Fe-Al-Ti-O system predicted by thermodynamic calculation included Al_2TiO_5, as a probable equilibrium phase in molten steel. However, there has been an experimental result showing the instability of Al_2TiO_5 in Ti-added ULC steel melts (Jo (2011)). Although the oxide stability diagram has been used to understand the inclusion evolution, published diagrams do not agree with each other and do not support experimental results on inclusion evolution. Therefore, the oxide stability of the Al-Ti complex inclusions has been a long-standing debate.

This is because the phase equilibria of the Fe-Al-Ti-O oxide system have not been fully investigated. The present authors recently carried out an experimental study on the phase equilibria in the Al-Ti-O system with an emphasis on the impact of oxygen partial pressure (Park *et al.* (2021)). Al_2TiO_5, which was shown to form a pseudobrookite solid solution with Ti_3O_5 should decompose under low oxygen partial pressure relevant to the molten steel during the secondary refining process. This indicates that it is no longer a stoichiometric oxide. The decomposition behaviour of Al_2TiO_5 may provide insights into the understanding of inclusion evolution in Ti-added ULC steel. However, for further application to Ti-added ULC steel, it is necessary to complete the modelling of the Fe-Al-Ti-O system, including both molten metal and several oxide phases in the system, in order to study the behaviour of complex inclusions in molten steel.

In the present study, thermodynamic modelling of the Fe-Al-Ti-O system was carried out to evaluate the stability of Al-Ti complex inclusions in Fe-Al-Ti-O melts. The evolution of Al-Ti complex inclusions in Ti-added ULC steel was also investigated using various methodologies including Scanning-Electron Microscopy with Energy-Dispersive X-ray Spectroscopy (SEM-EDS), Electron Back-Scattered Diffraction (EBSD), and Confocal Scanning Laser Microscopy (CSLM).

2. THERMODYNAMIC MODELLING OF THE FE-AL-TI-O SYSTEM

Thermodynamic calculations and optimization for the Fe-Al-Ti-O system were conducted using FactSage thermodynamic software (Bale *et al.* (2016)). The Gibbs energies of pure substances were sourced from the SGTE compilation of Dinsdale (1991). The Fe-Al-Ti-O system was modelled by considering solution phases such as liquid alloy, liquid oxide, pseudobrookite, cubic spinel, ilmenite, rutile, monoxide, some metallic solutions, and stoichiometric compounds. The modelling assessed various sub-binary systems and extended to multi-component systems to cover the entire subsystem of the Fe-Al-Ti-O system. In certain instances, model parameters were adjusted slightly to meet the requirements of the phase diagrams and thermodynamic properties of solutions. Details of the models and parameter optimization can be found elsewhere (Park and Kang (2024)).

2.1. Thermodynamic models

2.1.1. Liquid metal and liquid oxide

The Modified Quasichemical Model (Pelton *et al.* (2000), Pelton and Chartrand (2001)) was employed in modelling the liquid metal and the liquid oxide separately, aiming to consider Short-Range Ordering (SRO) observed in the liquid solutions across a broader concentration range. For example, in the case of liquid metal, components A, B, C, ... are distributed over a quasi-lattice as atoms. In the pair approximation, the pair-exchange reaction is considered as:

$$(A - A) + (B - B) = 2(A - B) \quad \Delta g_{AB} \tag{1}$$

where (A - A), (B - B), and (A - B) represent First-Nearest-Neighbor (FNN) pairs. The non-configurational Gibbs energy change for the formation of two moles of (A - B) pairs is Δg_{AB} which is used as a model parameter in each binary system. Gibbs energies of ternary and higher-order

systems are then estimated using the appropriate interpolation method (Pelton and Chartrand (2001)), and a few of adjustable ternary model parameters can be added. The Gibbs energy of liquid oxide phase was modelled similarly.

2.1.2. Solid solutions including pseudobrookite, ilmenite, cubic spinel, etc.

Solid phases having more than two sublattices such as pseudobrookite (($Ti,Al,Fe)_3O_5$), cubic spinel ($Fe(Al,Ti)_2O_4$)), and ilmenite (($Ti,Al,Fe)_2O_3$), etc. were modelled using the Compound Energy Formalism (CEF) (Hillert (2001)) to described the Gibbs energies of the solutions in the Fe-Al-Ti-O system. For example, the model for the Fe-Al-Ti-O pseudobrookite is described below:

$$(Fe^{2+}, Fe^{3+}, Ti^{3+}, Ti^{4+}, Al^{3+})^{4c}(Fe^{2+}, Fe^{3+}, Ti^{3+}, Ti^{4+}, Al^{3+})^{8f}_2O_5 \qquad [2]$$
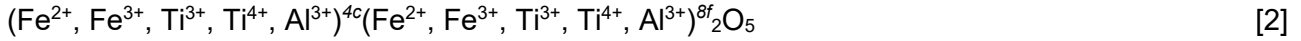
where ions enclosed in parentheses occupy the same octahedral (*4c* and *8f*) sublattice.

The Gibbs energy of the pseudobrookite solution is expressed as:

$$G^m = \sum_i \sum_j Y_i^{4c} Y_j^{8f} G_{ij} - TS^{\text{config}} + G^{\text{excess}} \qquad [3]$$

where Y_i^{4c} and Y_j^{8f} represent the site fractions of constituents '*i*' and '*j*' on the *4c* and *8f* octahedral sublattices, respectively; G_{ij} is the Gibbs energy of an 'end member $[i]^{4c}[j]^{8f}_2O_5$' in which *4c* and *8f* sites are occupied only by *i* and *j* cations, respectively; S^{config} is the configurational entropy which takes into account random mixing of cations on each sublattice. The Gibbs energies (G_{ij}) of end-members are the primary model parameters.

However, due to the presence of several non-neutral charged end-members, it is not feasible to ascertain the Gibbs energies of all end-members based solely on experimental data. To appropriately determine the values of these Gibbs energies, physically meaningful linear combinations of the end-members' Gibbs energies (G_{ij}) involved in specific site exchange reactions among cations are utilized as parameters in the model.

Taking the example of a Ti_3O_5 pseudobrookite oxide, the measurable Gibbs energy, $G^o(Ti_3O_5)$ (Gibbs energy of pure Ti_3O_5), is directly employed in the CEF modelling. The model parameters also encompass site exchange reactions between cations at the 4c and 8f sites, denoted by Δ and *I* parameters. These parameters are crucial in determining the Gibbs energies of end-members. Generally, these exchange energies are expected to be small and are frequently set to zero. This practice allows for a more controlled determination of the Gibbs energies of end-members, as opposed to arbitrary assignments without a rationale. Adopting this approach enhances the predictive capability and stability of the model, particularly for extensive solid solutions like pseudobrookite, ilmenite, and spinel phases.

The Gibbs energies of other solid phases without sublattice was described by a simple Bragg-Williams random mixing model.

2.2. Model calculation

Using the reported thermodynamic modelling of subsystems of the Fe-Al-Ti-O system, the present study extended the previous modelling to construct a model database for the Fe-Al-Ti-O system. Through model calculations of the Al-Ti-O oxide system, a definition of Al-Ti complex inclusions has been achieved. Considering the characteristics of Al_2TiO_5, formerly considered as an Al-Ti complex inclusion, the present study aimed to interpret the evolution and decomposition behaviours of Al-Ti complex inclusions under various oxygen pressure conditions (Section 2.2.1).

Additionally, deoxidation equilibria in Ti-added ULC steel were described by modelling the deoxidation equilibria by Al and by Ti. While the previous research conducted by Paek (Paek *et al.* (2016)), using MQM for the liquid metal phase was adopted, additional modelling of Ti-deoxidation equilibria was performed using MQM to provide a more refined interpretation of equilibrium relationships in Ti-added ULC steel production (Section 2.2.2).

At the final stage, the equilibrium [O] contents and corresponding inclusion phases in molten steel at 1600 °C were interpreted based on the Al and Ti contents in the liquid steel. Unlike the model calculations investigated previously, the model database optimized in the present study allows for the calculation of not only the oxide phases in equilibrium with ULC liquid steel but also the Fe, Al

and Ti solubilities within the oxide phase. This capability is expected to facilitate tracking the generation and transition behaviours of inclusions under reoxidation conditions.

2.2.1. Al-Ti-O oxide phase diagram at 1600 °C

The calculated result of the Al-Ti-O_2 phase diagram (P_{O2} - R_{Ti}) is shown in FIG 1. It should be stressed that there is a wide solid solution encompassing "Al_2TiO_5" (R_{Ti} = 0.33) and "Ti_3O_5" (R_{Ti} = 1.0) over a wide range of P_{O2} (1 - 10^{-14} atm), according to the present authors' experimental investigation (Park *et al.* (2021)). These two oxides have the same crystal structure, therefore, these were treated in a single solid solution (pseudobrookite s.s.). However, this solid solution separates into two phases at lower temperatures (T < 1500 °C), which was first revealed by the present authors (Park *et al.* (2021)). This kind of phase equilibrium has not been known previously. According to this phase equilibria, Al_2TiO_5 should undergo the following phase transformation at lower P_{O2} relevant to the steel refining process:

$$Al_2TiO_5 \text{ (at high } P_{O2}) \rightarrow (Ti,_{Al})_3O_5 + Al_2O_3 + O_2 \text{ (at low } P_{O2}) \qquad [4]$$
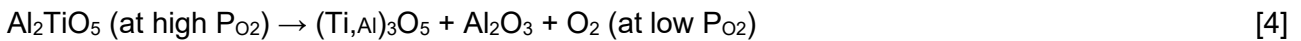
where "Al_2TiO_5 (at high P_{O2})" and "$(Ti,_{Al})_3O_5$" represent Al-rich pseudobrookite s.s. and Ti-rich pseudobrookite s.s., respectively. This reaction would represent a situation that Al-Ti complex inclusions (near Al_2TiO_5) generated at high oxygen potential due to reoxidation in Ti-added ULC steel could generate Ti-rich oxide inclusion, Al_2O_3, and the additional O in the liquid steel. This suggests that the oxide inclusion reoxidised in Ti-added ULC steel may play as an O-carrier in the liquid steel.
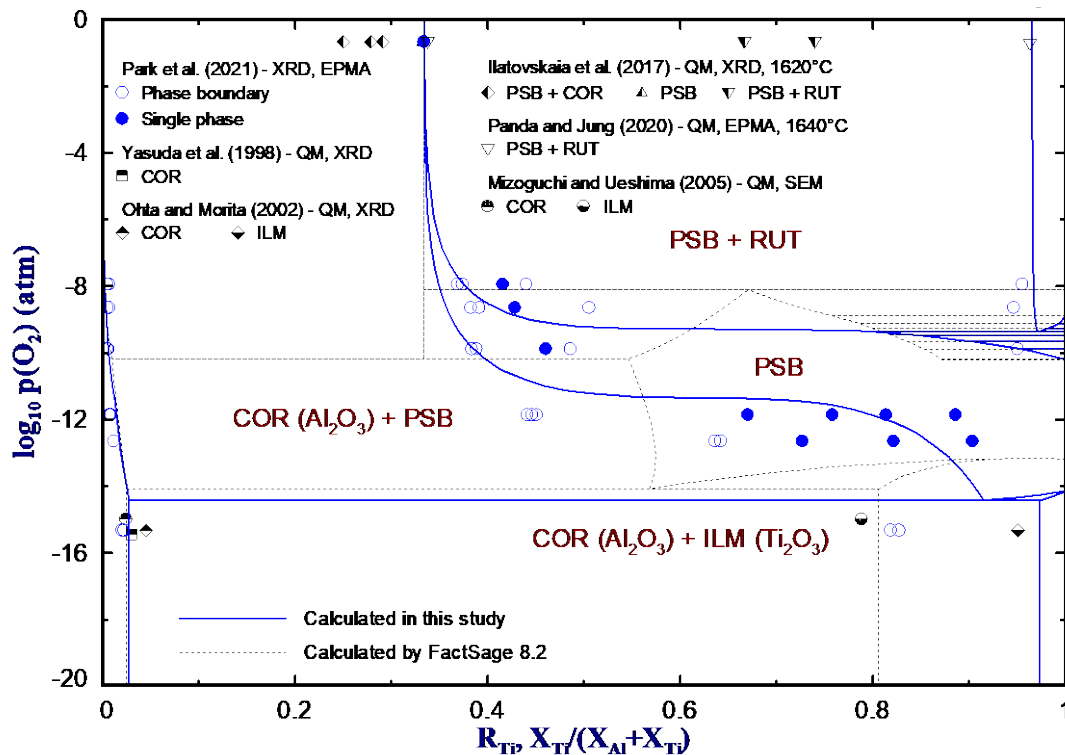
FIG 1. Calculated phase diagram of the Al-Ti-O_2 system at 1600 °C. Blue solid lines were calculated using the present thermodynamic model, and black dotted lines were calculated using FactSage FTOxid database. Symbols are the reported experimental data (see Park *et al.* (2021)).

These models were extended to incorporate Fe as a component. Detail modelling results can be found elsewhere (Park and Kang (2024)).

2.2.2. Ti deoxidation equilibria at 1600 °C

By combining the existing thermodynamic model of the Fe-Al-O liquid metal (Paek *et al.* (2016)), with that of the Fe-Ti-O liquid metal in the present study, the thermodynamic model for the deoxidation equilibria in the Fe-Al-Ti-O liquid metal could be completed. FIG 2 shows the Ti-deoxidation equilibria

4

in the liquid Fe-Ti-O at 1600 °C. Two thermodynamic calculations are shown: one calculation using WIPF (Cha *et al.* (2006)) and the other calculation using MQM in the present study. The present study describes the Ti-deoxidation equilibria over a wide composition range. The developed thermodynamic model is now used to predict high-temperature equilibria between Ti-added ULC steel and oxide inclusions.
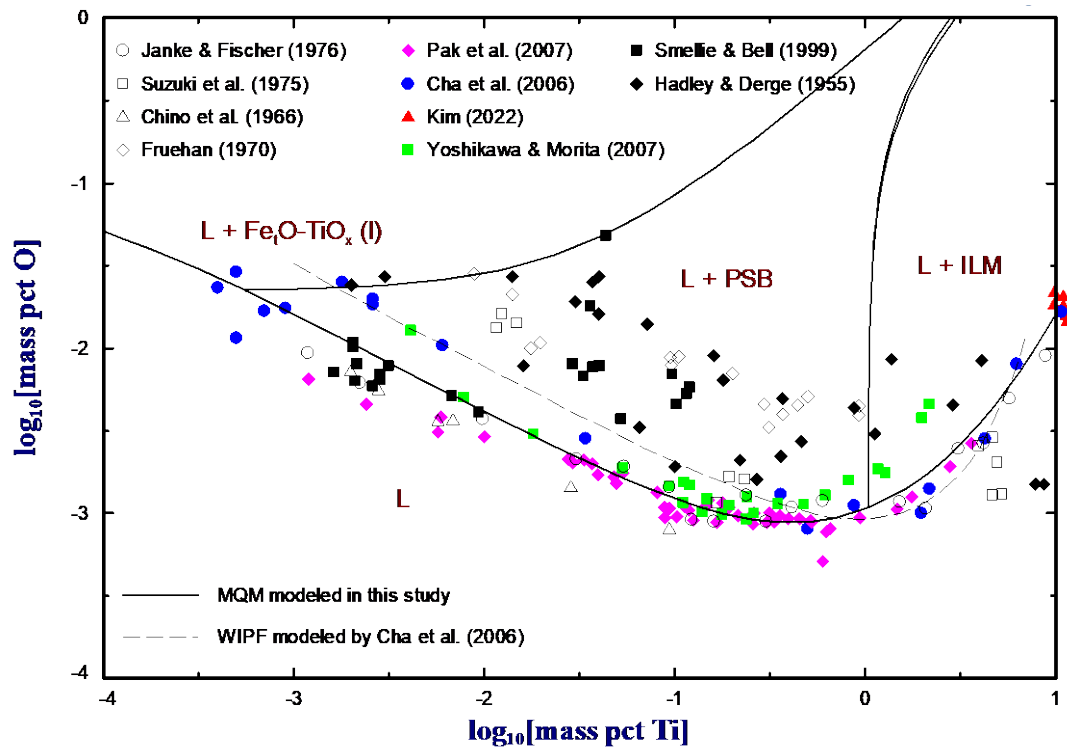
FIG 2. Ti-deoxidation equilibria in liquid iron at 1600 °C. Solid lines were calculated using the present thermodynamic model, and the dashed line was calculated using WIPF (Cha *et al.* (2006)).

2.2.3. Oxide stability diagram of the Fe-Al-Ti-O system

The calculated oxide stability diagram of the Fe-Al-Ti-O system at 1600 °C using the thermodynamic models developed in the present study is shown in FIG 3. Thin black solid lines and blue solid lines are the iso-O (ppm) lines, and the phase boundaries between two different oxide phases, respectively. The most probable oxide phase formed during the Ti-added ULC steel production is obviously Al_2O_3, by typical compositions of this steel grade. The red dashed lines are the phase boundary reported by Kang and Lee (Kang and Lee (2017)) in an earlier version of the present thermodynamic model. Compared to the previous stability diagram by Kang and Lee (Kang and Lee (2017)), the phase boundaries between corundum (Al_2O_3) and pseudobrookite oxide are similar to each other: no separate Al_2TiO_5 phase region is seen. However, the incorporation of Fe in the pseudobrookite s.s. resulted in a somewhat wider stability region of the pseudobrookite s.s. This subsequently resulted in the stability region of the liquid oxide and ilmenite (Ti_2O_3) phases being reduced.

5
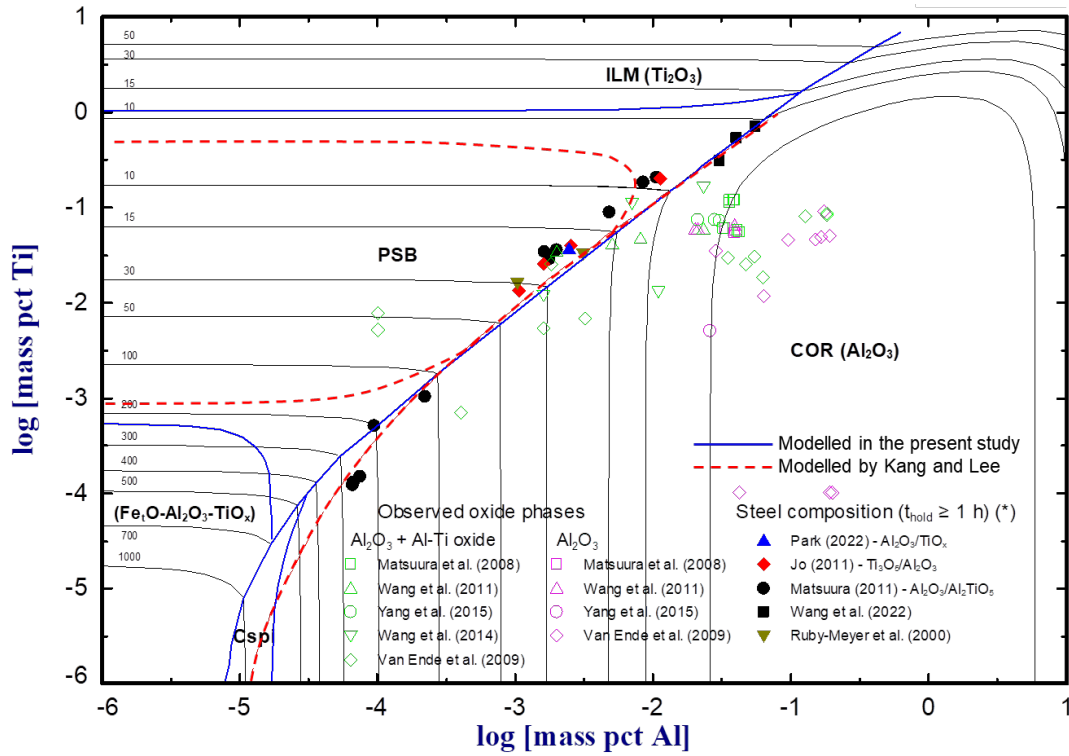
FIG 3. Calculated oxide stability diagram of the Fe-Al-Ti-O system at 1600 °C in the present study. Red dashed lines are taken from Kang and Lee (Kang and Lee (2017)). (*): the steel composition when reacted with specified oxides and kept for longer than 1 hour at 1600 °C.

3. EVOLUTION OF AL-TI COMPLEX INCLUSION IN LIQUID STEEL

Through the thermodynamic modelling of the Al-Ti-O system, the decomposition reaction of the Al-Ti complex oxide, as expressed in Reaction [4], was elucidated. Reaction [4] can be extended to the Fe-containing system, the Fe-Al-Ti-O system. In the reaction involving Fe, such as expressed in Reaction [5], the solubility of Fe in the pseudobrookite inclusion and the incorporation of the decomposition product O_2 into the molten steel can contribute to an increase in $\underline{O}$ contents.

$$(Fe,Al,Ti)_3O_5 \text{ (at high } P_{O2}) \rightarrow (Ti,_{Al})_3O_5 + Al_2O_3 + \underline{O} + Fe \text{ (at low } P_{O2}) \qquad [5]$$
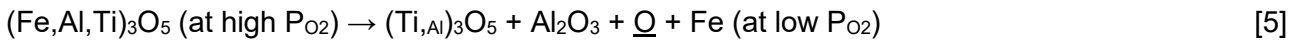
where "$(Fe,Al,Ti)_3O_5$ (at high P_{O2})" represents a reoxidised pseudobrookite s.s. The O generated in Reaction [5] can react with $\underline{Al}$ and/or $\underline{Ti}$ in the liquid steel to produce additional inclusions. The evolution and transition behaviours of Al-Ti complex inclusions, as depicted in FIG 4, may be considered. FIG 4(a) and (b) are the possible transition and decomposition behaviours of Al-Ti complex inclusions under different reoxidation conditions. In FIG 4(a) representing mild reoxidation conditions, the decomposition of $(Fe,Al,Ti)_3O_5$ leads to the generation of additional Al_2O_3 and an excess O source, $\underline{O}$. The $\underline{O}$ reacts with $\underline{Al}$ in the liquid steel, resulting in the creation of additional inclusions. In FIG 4(b) representing a severe reoxidation condition, $\underline{Al}$ and $\underline{Ti}$ content near the Al-Ti complex inclusion may be insufficient, leading to the oxidation of Fe, which can be incorporated into pseudobrookite s.s. The oxidation of Fe may cause additional troubles: reoxidation source as the O carrier, difficulty of separation from the liquid steel by floatation due to increased inclusion density, etc., potentially worsening steel cleanliness.

In order to verify the above predictions, some experiments using various experimental techniques were also carried out. The experimental results will be presented.

6
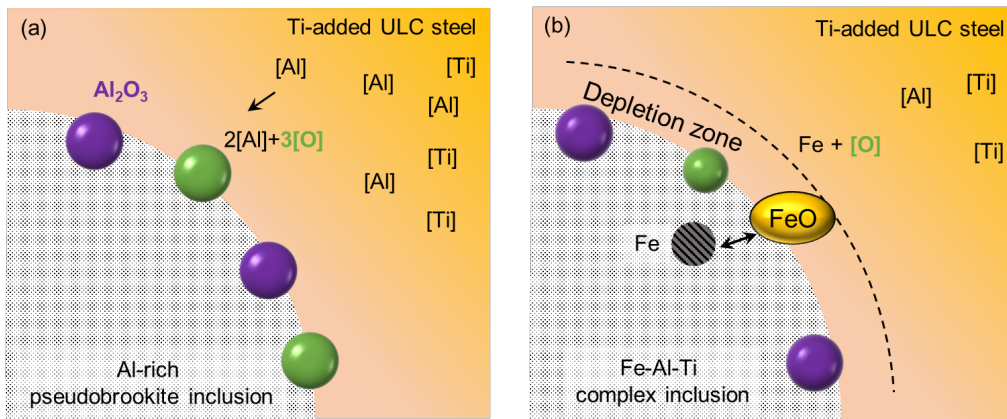
FIG 4. Schematic illustration of transition and decomposition behaviours of Al-Ti complex inclusions under (a) mild and (b) severe reoxidation conditions.

4. CONCLUSIONS

A self-consistent thermodynamic model of the Fe-Al-Ti-O system was developed, and the evolution of Al-Ti complex inclusions and their transition behaviours were investigated using various experimental techniques. It was shown that the Al-Ti complex inclusion should be defined as a part of pseudobrookite s.s. instead of the stoichiometric "Al_2TiO_5", which is not stable in liquid steel. The predicted transition behaviours of the Al-Ti complex inclusions were postulated, and it was demonstrated that the complex inclusions can act as a reoxidation source, potentially deteriorating steel cleanliness.

REFERENCES

Bai, X.-F., Sun, Y. and Zhang, Y. (2019) 'Transient evolution of inclusions during Al and Ti additions in Fe-20 Mass pct Cr alloy,' Metals, 9(6), p. 702. https://doi.org/10.3390/met9060702.

Bale, C.W. Bélisle, E., Chartrand, P., Decterov, S.A., Eriksson, G., Gheribi, A.E., Hack, K., Jung, I.-H., Kang, Y.-B., Melançon, J., Pelton, A.D., Petersen, S., Robelin, C., Sangster, J., Spencer, P., and Van Ende, M-A. (2016) 'FactSage Thermochemical Software and Databases, 2010–2016,' CALPHAD, 54, pp. 35–53. https://doi.org/10.1016/j.calphad.2016.05.002.

Basu, S., Choudhary, S. K., and Girase, N. U. (2004). Nozzle clogging behaviour of Ti-bearing Al-killed ultra low carbon steel. ISIJ International, 44(10), 1653–1660. https://doi.org/10.2355/isijinternational.44.1653.

Bernhard, C., Dorrer, P., Michelic, S. K., and Rössler, R. (2019). The role of FeTi addition to micro-inclusions in the production of ULC steel grades via the RH Process route. BHM Berg- Und Hüttenmännische Monatshefte, 164(11), 475–478. https://doi.org/10.1007/s00501-019-00900-2.

Cha, W.-Y, Nagasaka, T., Miki, T., Sasaki, Y., and Hino, M. (2006) 'Equilibrium between titanium and oxygen in liquid Fe-Ti alloy coexisted with titanium oxides at 1873 K,' ISIJ International, 46(7), pp. 996–1005. https://doi.org/10.2355/isijinternational.46.996.

Cui, H., Bao, Y., Wang, M., and Wu, W. (2010). Clogging behavior of submerged entry nozzles for Ti-bearing IF steel. International Journal of Minerals, Metallurgy and Materials, 17(2), 154–158. https://doi.org/10.1007/s12613-010-0206-y.

Dinsdale, A.T. (1991). SGTE data for pure elements. Calphad, 15(4), pp. 317–425. https://doi.org/10.1016/0364-5916(91)90030-n.

Dorrer, P., Michelic, S. K., Bernhard, C., Penz, A., & Rössler, R. (2019). Study on the influence of FeTi-addition on the inclusion population in Ti-stabilized ULC steels and its consequences for SEN-clogging. Steel Research International, 90(7). https://doi.org/10.1002/srin.201800635.

Fukuda, N. (1973) 'Manufacture of Ti-stabilized extra low carbon steel for deep drawing quality.' Tetsu-to-Hagane, 59(2), pp. 231–240.

Gupta, I., and D. Bhattacharya. (1989) 'Metallurgy of formable vacuum degassed interstitial-free steels.'

Hillert, M. (2001) 'The compound energy formalism,' Journal of Alloys and Compounds, 320(2), pp. 161–176. https://doi.org/10.1016/s0925-8388(00)01481-x.

Jo, J.O. (2011) 'Thermodynamics of Titanium and Aluminum in Liquid Alloy Steel,' PhD dissertation, Hanyang University.

Kang, Y.-B. and Lee, J.-H. (2017) 'Reassessment of oxide stability diagram in the Fe–Al–Ti–O system,' ISIJ International, 57(9), pp. 1665–1667. https://doi.org/10.2355/isijinternational.isijint-2017-182.

Lee, J., Kang, M., Kim, S., Kim, J., Kim, M., & Kang, Y. (2019). Influence of Al/Ti ratio in Ti-ULC steel and refractory components of submerged entry nozzle on formation of clogging deposits. ISIJ International, 59(5), 749–758. https://doi.org/10.2355/isijinternational.isijint-2018-672.

Matsuura, H., Tsukihashi, F. (2012) 'Compositional and morphological control of non-metallic inclusions in Fe–Al–Ti alloy,' Proc. Clean Steel in the Future – Prof. Hae-Geon Lee Symposium, Korean Inst. Met. Mater., pp. 14–26.

Park, Y.-J, and Kang, Y.-B. (2024) 'Thermodynamic modelling of the Fe-Al-Ti-O system,' unpublished work, POSTECH.

Park, Y.-J., Kim, W.-Y. and Kang, Y.-B. (2021) 'Phase equilibria of Al_2O_3–TiO_x system under various oxygen partial pressure: Emphasis on stability of Al_2TiO_5–Ti_3O_5 pseudobrookite solid solution,' Journal of the European Ceramic Society, 41(14), pp. 7362–7374. https://doi.org/10.1016/j.jeurceramsoc.2021.06.052.

Paek, M., Jang, J., Pak, J. and Kang, Y.-B. (2015) 'Aluminum Deoxidation Equilibria in liquid iron: Part I. Experimental,' Metallurgical and Materials Transactions B-process Metallurgy and Materials Processing Science, 46(4), pp. 1826–1836. https://doi.org/10.1007/s11663-015-0368-0.

Paek, M., Pak, J. and Kang, Y.-B. (2015) 'Aluminum deoxidation equilibria in liquid iron: Part II. Thermodynamic Modeling,' Metallurgical and Materials Transactions B-process Metallurgy and Materials Processing Science, 46(5), pp. 2224–2233. https://doi.org/10.1007/s11663-015-0369-z.

Pelton, A.D., Degterov, S.A., Eriksson, G., Robelin, C., and Dessureault, Y. (2000) 'The modified quasichemical model I—Binary solutions,' Metallurgical and Materials Transactions B-process Metallurgy and Materials Processing Science, 31(4), pp. 651–659. https://doi.org/10.1007/s11663-000-0103-2.

Pelton, A.D. and Chartrand, P. (2001) 'The modified quasi-chemical model: Part II. Multicomponent solutions,' Metallurgical and Materials Transactions A, 32(6), pp. 1355–1360. https://doi.org/10.1007/s11661-001-0226-3.

Wang, C., Nuhfer, N. T., and Sridhar, S. (2009). Transient behavior of inclusion chemistry, shape, and structure in Fe-Al-Ti-O melts: effect of titanium source and laboratory deoxidation simulation. Metallurgical and Materials Transactions B-process Metallurgy and Materials Processing Science, 40(6), 1005–1021. https://doi.org/10.1007/s11663-009-9267-6.